International Seminar on Student Research in Education, Science, and Technology
ISSN 3047-1532 | Volume 2 April 2025, pp. 199-212

https://www.issrestec.id/
http://journal.ummat.ac.id/index.php/issrestec
Universitas Muhammadiyah Mataram, Indonesia

The Effect of Liquid Superficial Velocity on Two-Phase Air-Water Slug Flow in a Horizontal Pipe Using High-Speed Camera

Resky Gerhana Hidayatullah[1], Syaiful Tambah Putra Ahmad[2], Akhmad Afandi[3], Khasani[4], Yusnita[5], Deendarlianto[6]
[1,2,4,6]Department of Mechanical and Industrial Engineering, Universitas Gadjah Mada, Yogyakarta, Indonesia
[3]Department of Mechanical Engineering, Politeknik Negeri Banyuwangi, Indonesia
[5]Study Program of Mechanical Automotive, Universitas Muhammadiyah Riau, Indonesia
gerhanaresky@gmail.com[1], syaifultpa@gmail.com[2], akhmad.afandi@poliwangi.ac.id[3], khasani@ugm.ac.id[4], jusnita@umri.ac.id[5], deendarlianto@ugm.ac.id[6]

Abstract: This study examines the impact of liquid superficial velocity (JL) on liquid slug length in two-phase air-water flow within a horizontal pipe. Experiments utilizing high-speed imaging were conducted to analyze slug length at different JL values while maintaining a constant gas superficial velocity (JG). Results show that increasing JL reduces slug length due to enhanced shear forces and turbulent interactions between the gas and liquid phases. At low JL, slugs are longer and exhibit high inter-slug variation, whereas at high JL, slugs become shorter and more uniform. Analysis of the slug length distribution reveals that the log-normal probability density function (PDF) effectively represents the trend, particularly at high JL, where slug fragmentation is more pronounced. The empirical model developed accurately predicts slug length, with most data falling within a ±25% error margin. Additionally, the average liquid slug length is 60% smaller than the maximum length and will never exceed this value, while the minimum slug length can decrease up to 630% of the average. These findings provide new insights into slug flow dynamics and offer valuable reference points for future studies on two-phase gas-liquid flow.

Keywords: Two Phase Flow, Slug Flow, Slug Length, Superficial Velocity.

Article History:
Received: 23-04-2025
Online : 25-04-2025

This is an open access article under the CC–BY-SA license

A. INTRODUCTION

Two-phase gas-liquid flow is a complex phenomenon commonly encountered in various industrial processes, such as petroleum production, thermal power plants, and chemical processes (Yeoh & Joshi, 2023). One of the main flow patterns in two-phase flow within horizontal pipes is slug flow, characterized by alternating liquid slugs and elongated gas bubbles (Deendarlianto et al., 2016). The study of slug flow is essential because it affects pressure distribution (Dinaryanto et al., 2017), heat transfer (Kusumaningsih et al., 2025), and the potential erosion of pipe walls, which in turn can influence operational efficiency (Zheng et al., 2008).

Previous studies, as shown in Table 1, generally highlight parameters such as pipe diameter, slug frequency, and liquid hold-up. However, fluctuations in slug length, an important aspect, are often overlooked despite their significant influence on transient pressure, mass transfer rate, and separator performance, making slug length fluctuations an essential parameter worthy of further investigation.

Table 1. Previous Researchers' Slug Length Measurement Equations

Author	Equation
(Brill, Schmidt, Coberly, Herring, & Moore, 1981)	$\ln\ \bar{L}_S = -2.663 + 0.059\ln\ v_M + 5.441(\ln\ d)^{0.5}$
(Norris, 1982)	$\ln\ \bar{L}_S = -2.099 + 4.859(\ln\ d)^{0.5}$
(Scott, Shoham, & Brill, 1989)	$\ln\ \bar{L}_S = -25.4 + 28.5(\ln\ d)^{0.1}$
(E. M. Al-Safran, Gokcal, & Sarica, 2013)	$\frac{L_S}{d} = 2.63\left(\frac{d^{3/2}\sqrt{\rho_L(\rho_L-\rho_G)g}}{\mu_L}\right)^{0.321}$
(Wang, 2012)	$\frac{L_S}{d} = \left\{10.1 + \frac{16.8}{1+\exp\left[-3.57\ln\left(\frac{d^2\sqrt{\rho_L(\rho_L-\rho_G)g}}{\mu_L}\right)+19.278\right]}\right\}\left(\cos^2\ \theta + \frac{\sin^2\theta}{2}\right)$
(Baba et al., 2018)	$\frac{L_S}{d} = 3.35\left(\frac{v_M}{\sqrt{gd}}\right)^{0.03}\left(\frac{d^{3/2}\rho_M\sqrt{g}}{\mu_L}\right)^{0.2}\left(\frac{\rho_M v_M d}{\mu_L}\right)^{0.1}$
(Shaaban & Al-Safran, 2023)	$\bar{L}_S = \frac{1}{F_S}\left[v_{TB} - \frac{v_{SG} - v_{GLS}(1-H_{LLS})}{H_{LLS} - H_{LTB}}\right]$

Superficial velocity is a key parameter in determining two-phase flow patterns. Variations in liquid superficial velocity (JL) significantly impact slug length, liquid fraction, and slug frequenc. The development of numerical models in slug flow simulations Budiana et al. (2020) has demonstrated good capability in addressing two-phase flow problems. However, numerical models still have limitations in accurately representing the complexity of the phenomenon. Therefore, experimental studies remain necessary to obtain high-quality data, which not only enrich understanding of slug flow characteristics but also serve as validation for numerical prediction results. Thus, this study highlights the relationship between liquid superficial velocity and slug length in two-phase air-water flow within horizontal pipes.

This research aims to explore the relationship between JL and liquid slug length under various conditions, including constant gas superficial velocity (JG) and varying JL conditions. The study focuses on understanding the dynamics of slug length resulting from changes in flow parameters, aiming to provide an in-depth understanding of slug flow phenomena. With a structured experimental approach and careful data analysis, this study offers new insights that can be utilized to enhance efficiency and safety of pipeline systems in various industrial applications.

B. METHOD

The experiments were conducted at the Horizontal Two-Phase Flow Facility (HORTOFF) located at the Department of Mechanical and Industrial Engineering, Universitas Gadjah Mada. This facility is designed to investigate the characteristics of two-phase gas-liquid flow in a horizontal pipe configuration. Details regarding the equipment and experimental procedures have been described in previous publications (Setyawan et al., 2017; Wijayanta et al., 2023; Wijayanta et al., 2022), and thus, only the main aspects of the equipment used are presented in this study. Figure 1 shows a schematic illustration of the experimental system used in this study. The system consists of a transparent acrylic pipe with an inner diameter of 26 mm and a total length of 10,000 mm, with the observation point located 5,200 mm from the mixer outlet. The choice of this observation point ensures that the flow conditions have reached stability before recording. The fluid used in these experiments is dry air as the gas phase and pure water (H_2O) as the liquid phase.

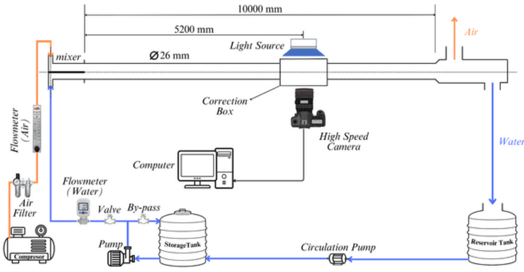

Figure 1. Schematic of the Research Setup.

To ensure accurate flow rate control, a centrifugal pump is used for water flow, and a centrifugal compressor is used for air flow. The water flow rate is controlled using an Omega brand rotameter with a capacity range of 1 to 10 LPM and an accuracy of ±2%, while the air flow rate is controlled using two Dwyer brand air rotameters with maximum capacities of 200 SCFH and 600 SCFH. The experiments are conducted under atmospheric pressure and room temperature conditions to ensure system stability and minimize the influence of external factors on the experimental results.

Flow visualization is performed using a high-speed video camera, the Phantom Miro M310, set at a frame rate of 240 fps, a resolution of 1024 × 200 pixels, and an exposure time of 15 µs. The camera is positioned at the observation point to record the motion of liquid slugs and gas bubbles within the pipe. To reduce optical distortion caused by the refractive index difference between air and acrylic material, a transparent acrylic box containing water is installed around the observation area. The use of water in this box is aimed at matching the refractive index with the pipe material, thereby improving image clarity. Additionally, a series of LED lights are used as supplementary light sources to ensure adequate exposure during each recording. In the two-phase flow analysis based on image processing, image calibration is necessary to convert the length from pixels to actual physical units. Calibration is performed by determining the conversion ratio (Cr), which is calculated based on a reference object of known real dimensions using Equation 1.

$$Cr = \frac{L_{actual}}{L_{pixels}} \tag{1}$$

After the conversion ratio ($Cr = 0.299$ mm/pixel) is obtained, the length of other objects in the image can be calculated using Equation 2.

$$L_{actual} = L_{pixels} \times Cr \tag{2}$$

In the experiments, this method is applied by using the outer diameter of the pipe as the reference. Recording is conducted for approximately 20 seconds, and the recorded images are extracted into an image sequence and converted into real units using Cr. The liquid slug length (L_{LS}) can be calculated using Equation 3 (Widyatama et al., 2018).

$$L_{LS} = X_n - X_t \tag{3}$$

Where X_n is the axial position of the liquid slug nose and X_t is the axial position of the liquid slug tail. In cases where the liquid slug length exceeds the length of the observation area, Equation 4 is used:

$$L_{LS} = (X_t - X_n) \times Cr + \left(\frac{U_{LS}}{FR}\right) \times (\Delta F) \tag{4}$$

$$U_{LS} = \Delta X_{n/t} \times \frac{FR}{\Delta Frame} \times \frac{d_m}{d_{pix}} \tag{5}$$

Where L_{LS} is the liquid slug length (m), U_{LS} is the liquid slug velocity (m/s), ΔF is the number of frames during the motion, FR is the camera frame rate (fps), d_m is the inner diameter of the pipe, and d_{pix} is the image height (pixel). To find the liquid slug velocity, Equation 5 is used. In addition to determining the slug length, this study also analyzes the slug frequency, which is defined as the number of slugs passing the observation point in a specific time interval. Mathematically, the slug frequency (f_s) can be calculated using Equation 6.

$$f_s = \frac{N_s}{T} \tag{6}$$

N_s is the number of slugs detected in the time period (T). In high-speed imaging experiments, T can be calculated from the number of frames used to observe the flow divided by the camera frame rate (fps), i.e.

$$T = \frac{\Delta F}{FR} \tag{7}$$

If the number of slugs passing the observation point during this period is N_s, then the slug frequency can be determined using Equation 8.

$$f_s = \frac{N_s \times FR}{\Delta F} \tag{8}$$

Slug frequency becomes an important parameter in characterizing slug flow dynamics because it is closely related to momentum transfer rate and pressure distribution in the pipe. This technique ensures that data obtained from high-speed imaging can be analyzed quantitatively with a high level of accuracy.

Figure 2 shows the data acquisition area based on the flow map by Mandhane et al. (1974)(Mandhane, Gregory, & Aziz, 1974), which is used to determine the JG and JL ranges in this experiment. With a systematic experimental approach and the use of high-speed imaging, this study aims to provide deeper insights into the liquid slug length characteristics in two-phase gas-liquid flow in horizontal pipes.

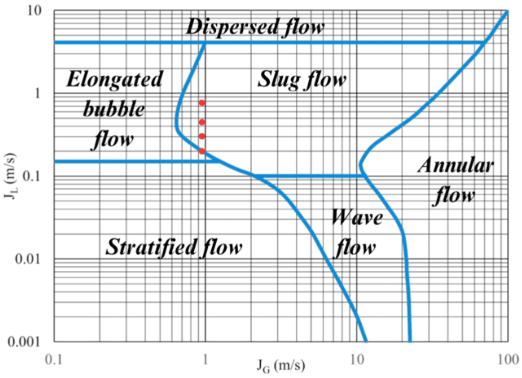

Figure 2. Research Region Range on the Mandhane et al. Flow Map(Mandhane et al., 1974).

Slug flow in horizontal pipes consists of liquid slugs and elongated gas bubbles as shown in Figure 3. Between two liquid slugs, there are elongated gas bubbles surrounded by a thin liquid film along the pipe wall. Additionally, tiny bubbles are dispersed in the liquid phase, formed due to friction and turbulent interactions between the gas and liquid phases. This flow forms a periodic pattern called a unit cell, which consists of one liquid slug followed by one elongated gas bubble. This flow structure is a characteristic feature of slug flow in two-phase gas-liquid systems and greatly influences pressure distribution and momentum transfer in the pipe.

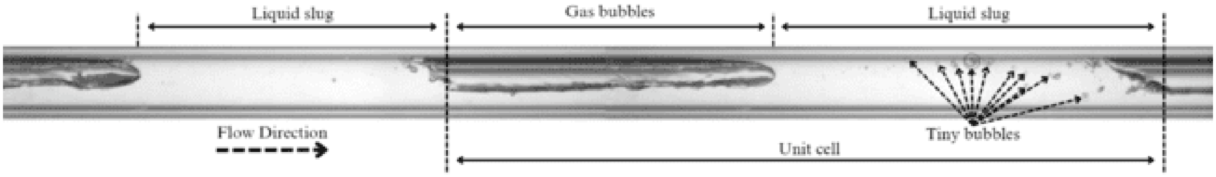

Figure 3. Slug Flow Structure

C. RESULTS AND DISCUSSION

The analysis was conducted based on data from recordings at various JL values with a constant JG. The results of slug length measurements are presented in graphical form and empirical distributions, which are compared with the log-normal model. Additionally, fluctuations in slug length for each variation in JL velocity are discussed to provide an understanding of the flow dynamics.

1. Visual

The visual results of the liquid slug flow structure were classified into three groups based on length: the highest length group (high positive fluctuation), the average length group (fluctuations approaching zero), and the shortest length group (high negative fluctuation), as shown in Table 2. Each group represents the characteristics of the liquid slug structure detected during the recordings.

In the highest length group, the liquid slug structure appears elongated with a low void fraction. The distribution of tiny bubbles is minimal, indicating relatively stable gas-liquid interaction. The flow structure in this group reflects a well-developed slug pattern with a clear unit cell pattern, consisting of one liquid slug followed by one elongated gas bubble.

Table 2. Liquid Slug at JG = 0.94 m/s with Maximum, Average, and Minimum Length Values

J_L (m/s)	**Visual**
0.2	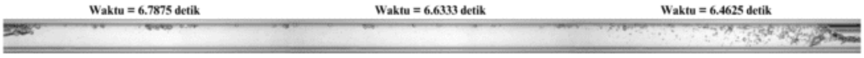 Length 0.9356 m (Fluctuations 39.93 %)
	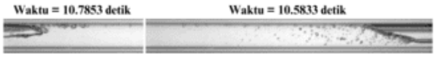 Length 0.5667 m (Fluctuations 0.83 %)
	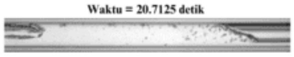 Length 0.2296 m (Fluctuations -144.68 %)
0.3	 Length 0.6394 m (Fluctuations 43.37 %)
	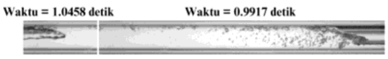 Length 0.3568 m (Fluctuations -1.46 %)
	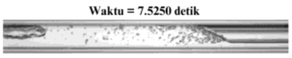 Length 0.0505 m (Fluctuations -615.81 %)
0.44	 Length 0.7068 m (Fluctuations 57.25 %)
	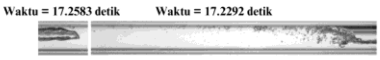 Length 0.3074 m (Fluctuations 1.73 %)
	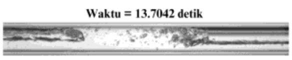 Length 0.1344 m (Fluctuations -124.79 %)
0.77	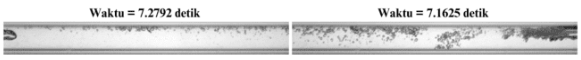 Length 0.6295 m (Fluctuations 54.23 %)
	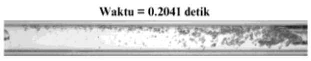 Length 0.2973 m (Fluctuations 3.07 %)
	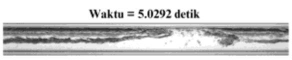 Length 0.0654 m (Fluctuations -340.589 %)

In the average-length group, the liquid slug is shorter compared to the first group, with an increased void fraction caused by the appearance of more tiny bubbles in the liquid phase. The appearance of these small bubbles indicates an increase in turbulence due to strong interactions between the gas and liquid phases. However, the unit cell pattern remains visible, indicating a relatively clear slug structure, despite beginning to experience fragmentation. Conversely, in the shortest length group, the liquid slug structure undergoes significant fragmentation, characterized by a drastic increase in void fraction and a broader distribution of tiny bubbles. Increased turbulence results in a less distinct flow structure, and this instability reflects the high interaction between the gas and liquid phases, which can cause the liquid slug to break apart or initiate into smaller segments.

An increase in JL significantly influences the structure of slug length. In general, as JL increases, the liquid slug length tends to decrease due to the increased shear force that accelerates slug fragmentation. Furthermore, increasing JL intensifies turbulent interactions, shown by an increase in the number of tiny bubbles and void fraction. These conditions cause the slug structure to become more complex.

The pattern of slug structure changes is clearly visible in each JL variation. At low JL (0.2 m/s), the liquid slug has a relatively large length with a stable structure, reflecting a well-developed slug pattern. At JL 0.3 m/s, the slug length decreases along with an increase in the number of tiny bubbles, indicating a structural transition due to increased turbulence. At JL 0.44 m/s and 0.77 m/s, the slug length decreases more significantly and becomes more extreme, with the widespread distribution of tiny bubbles indicating flow instability due to increasingly intense interactions between gas and liquid.

2. Length and frequency

The relationship between the average liquid slug length and slug frequency as a function of JL at a constant JG = 0.94. The measurement results indicate that an increase in JL has a significant effect on both parameters. At JL = 0.2 m/s, the average slug length reaches its highest value of approximately 0.562 m, with a low slug frequency of 0.28 Hz. This condition suggests that at low velocity, slugs tend to be longer, reflecting a classic slug flow with a clear unit cell pattern. However, as JL increases to 0.3 m/s, the average slug length sharply decreases to about 0.362 m, while the slug frequency increases to 0.52 Hz. This drastic reduction in slug length indicates faster slug fragmentation due to the increased shear force between the gas and liquid phases. The increase in slug frequency at this condition indicates that the time interval between slugs shortens as more slug unit cells form within the same time period.

At JL = 0.44 m/s and 0.77 m/s, the average slug length decreases only slightly, to around 0.302 m and 0.288 m, respectively. However, slug frequency continues to increase significantly, reaching a peak value of 2.10 Hz at JL = 0.77 m/s. The sharp rise in slug frequency indicates that the rate of slug formation is increasing, so the number of slugs passing through the observation point within a given time increases exponentially. This phenomenon reflects the increasing turbulence at the gas-liquid interface, which accelerates the process of forming new slugs. Furthermore, the high slug frequency at high JL may lead to more frequent transient pressure fluctuations (slug-induced pressure fluctuations) Dinaryanto et al. (2017), thus increasing the risk of fatigue failure in the pipe walls.

The pattern of changes in slug length and slug frequency also reveals several more complex physical phenomena. First, there is a contrast in the patterns of changes in slug length and slug frequency. The decrease in slug length, accompanied by a sharp increase in slug frequency, suggests a transition from long and infrequent slug flows to shorter and more frequent slugs. Second, an asymptotic phenomenon in the average slug length is observed, where, at JL = 0.44 m/s to 0.77 m/s, slug length tends to remain constant despite an increase in JL. This indicates that at a certain point, slug length reaches an equilibrium between shear force and differential pressure, so that further increases in JL no longer significantly affect slug length, but instead predominantly increase slug frequency, as shown in Figure 4.

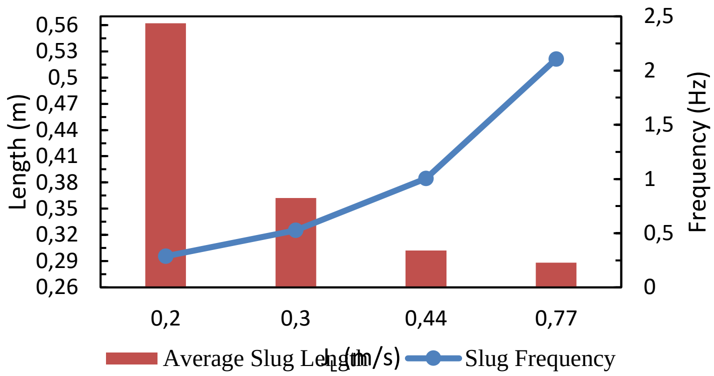

Figure 4. Average Liquid Slug Length and Frequency at JG = 0.94 m/s

Additionally, the pattern of increasing slug frequency shows non-linear behavior, where the increase in frequency within the JL range of 0.3 to 0.77 m/s is much more significant compared to the transition from 0.2 to 0.3 m/s. This suggests the existence of a threshold for the kinetic energy of the liquid phase, beyond which slug formation accelerates, becoming more frequent. This threshold occurs due to an increase in the instability of the gas-liquid interface, which develops into consecutive slugs. The increase in JL also causes significant changes in the liquid hold-up volume, reflected by the decrease in average slug length. As JL increases, the volume of liquid trapped in the slugs decreases, due to intensified turbulent interactions that push the liquid more quickly downstream.

3. Fluctuations

The variation of liquid slug length with slug number at different JL values, providing a comprehensive overview of the slug length dynamics during the recording process. At JL = 0.2 m/s, the slug length tends to be larger, with a maximum value of approximately 0.935 m and a minimum of 0.229 m. Moreover, the variation in length between slugs shows significant differences compared to other JL conditions. This phenomenon suggests that at low JL, the slugs formed tend to be larger but more irregular, likely due to the dominance of gravitational wave effects in the horizontal pipe.

At JL = 0.3 m/s, the slug length begins to decrease, with maximum and minimum values of approximately 0.639 m and 0.050 m, respectively. Although the variation in slug length remains relatively high, these values are lower than those observed at JL = 0.2 m/s. This reduction in slug length indicates increased turbulence, which causes faster fragmentation of the slug, resulting in a smaller variation in slug length compared to lower JL conditions, as shown in Figure 5.

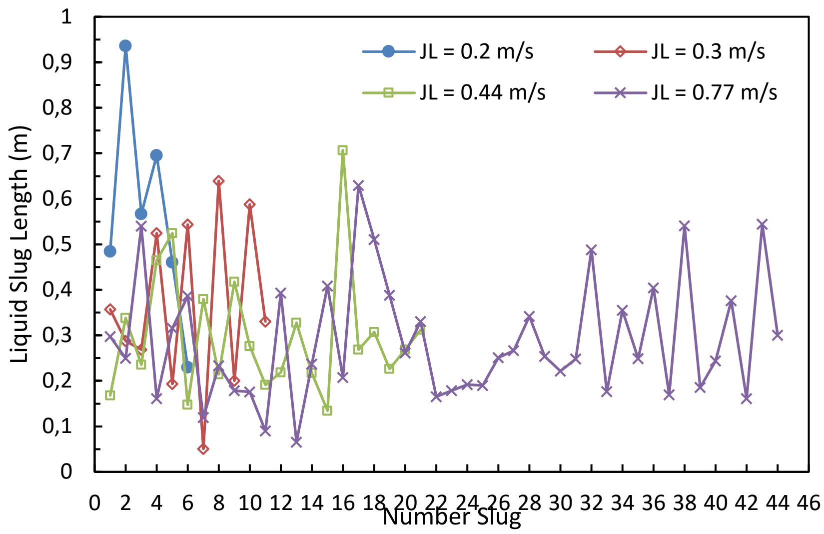

Figure 5. Liquid Slug Length at JG = 0.94 m/s Detected Over 20 Seconds

As JL increases to 0.44 m/s, the slug length pattern shows gradual changes, as observed in slug numbers 9-10-11, 13-14-15, and 19-20-21. This phenomenon is rarely seen at JL = 0.2 m/s and 0.3 m/s. The gradual change in slug length suggests stable slug distribution during its movement. The maximum and minimum slug lengths are around 0.706 m and 0.1344 m, respectively, indicating that at medium JL, the interaction between the gas and liquid phases intensifies, contributing to the formation of tiny bubbles within the liquid slug.

At the highest JL, 0.77 m/s, the average slug length becomes shorter, with maximum and minimum values of approximately 0.629 m and 0.065 m, respectively, accompanied by an increased number of detected slugs. The gradual changes in slug length are more frequently observed, as seen in slug numbers 4-5-6, 8-9-10-11, 17-18-19-20, and 25-26-27-28. Even at slug numbers 22-23-24-25, the liquid slug length distribution appears to be very stable. In general, the variation in liquid slug length between JL = 0.44 m/s and 0.77 m/s is not significant but still lower than those observed at JL = 0.2 m/s and 0.3 m/s. Overall, the variation pattern of slug lengths at different JL values still shows sporadic occurrences of maximum and minimum slug lengths. This indicates the continued instability in the two-phase flow, influenced by the dynamics of gas-liquid interactions during the slug's movement.

The fluctuation pattern of slug length relative to the average slug length value. The data obtained shows that each JL generates a trend curve that is nearly similar in distribution pattern, though still separated and not overlapping. This phenomenon suggests that the relationship between slug length and its fluctuations is systematic and specific for each JL value, thus allowing for the prediction of slug length, JL, and its fluctuations by following the trend curve pattern, as shown in Figure 6.

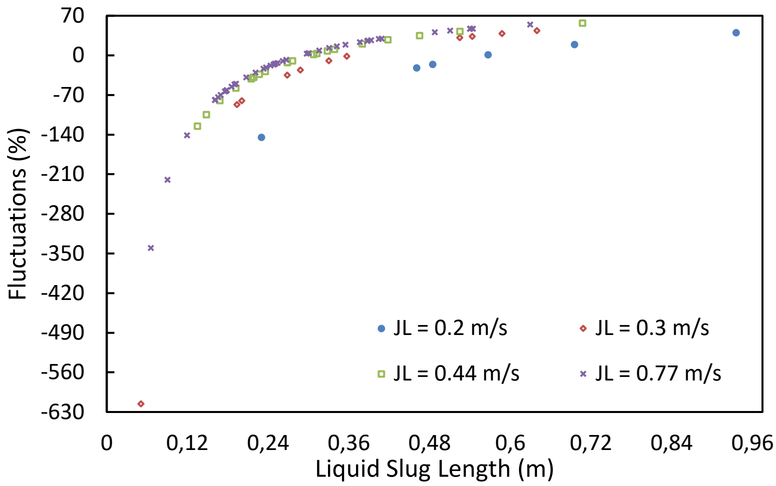

Figure 6. Fluctuations in Liquid Slug Length from the Average Value at JG = 0.94 m/s

The uniqueness of the pattern formed for each JL lies in the similarity of the trend curve shapes, but still separated without overlap. This indicates that while the relationship between slug length, JL, and fluctuations exhibits a similar regularity, each JL has a distinct distribution, allowing for specific identification of its characteristics. Thus, when two out of the three parameters (JL, slug length, or fluctuation) are known, an empirical equation can be used to mathematically determine the unknown parameter. The consistency of the trend curves emphasizes that the relationship between slug length, JL, and fluctuations is not random but follows a systematic pattern that can serve as the foundation for further modeling.

4. Modeling

The distribution of liquid slug length at various JL values, compared with the log-normal distribution model as a probabilistic approach. Each sub-graph displays the slug length distribution pattern with a tendency for changes in distribution characteristics as JL increases. At low JL, as seen in sub-graphs (a) and (b), the slug length distribution shows a wider spread with higher mode values. This indicates that larger slugs are more likely to form under low JL conditions, reflecting a slug flow pattern with longer liquid slugs. In contrast, at higher JL, as seen in sub-graphs (c) and (d), the slug length distribution shifts towards smaller values with a more concentrated distribution. This phenomenon suggests that an increase in JL leads to faster slug fragmentation, resulting in shorter and more uniform slug lengths, as shown in Figure 7.

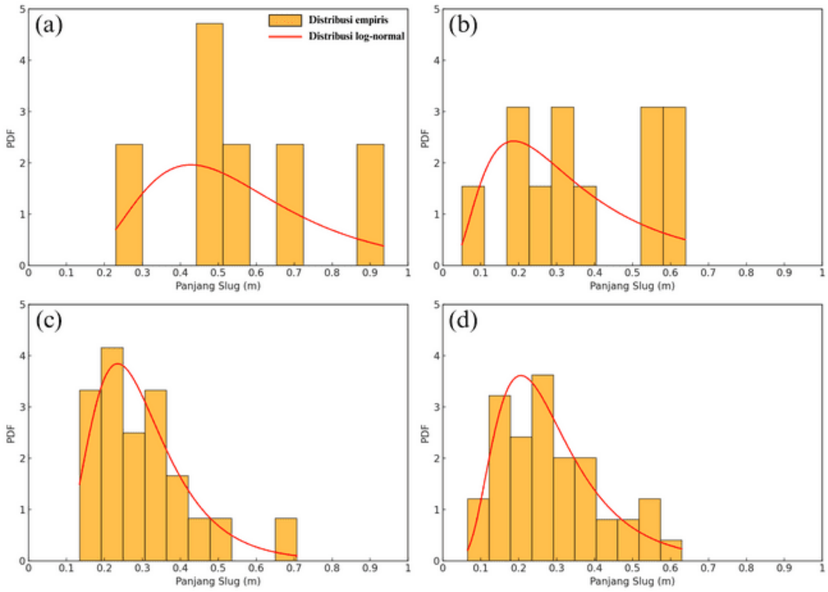

Figure 7. Liquid Slug Length Statistics at JG = 0.94 m/s: (a) Empirical and Log-Normal Distribution for JL = 0.2 m/s; (b) Empirical and Log-Normal Distribution for JL = 0.3 m/s; (c) Empirical and Log-Normal Distribution for JL = 0.44 m/s; (d) Empirical and Log-Normal Distribution for JL = 0.77 m/s

The alignment between empirical data and the log-normal model also shows an interesting pattern. At low JL, there is a larger deviation between the empirical distribution and the log-normal curve, particularly in the higher slug length range. This indicates that the slug length distribution is more varied at low JL, likely due to the dominance of gravitational forces allowing slugs to grow longer. Conversely, at high JL, the slug length distribution becomes more symmetrical and closer to the log-normal distribution, indicating that more intense slug fragmentation results in more uniform slug lengths.

The empirical distribution at low JL also shows a long tail pattern, indicating that extreme slug lengths occur more frequently than predicted by the log-normal model. In contrast, at high JL, the distribution is more concentrated around the mode value, suggesting that increased JL results in more uniform slug lengths due to the dominant effects of shear forces and turbulence. Thus, the log-normal model is able to represent the slug length distribution trend quite well, particularly at high JL conditions, where slug fragmentation is more intense and the slug length distribution is more stable. This suggests that probabilistic models like log-normal can be used to describe the characteristics of slug length distribution, particularly under more turbulent flow conditions with significant slug fragmentation.

Comparison between model predictions and experimental laboratory data in determining the liquid slug length. The proposed model was developed based on an empirical relationship connecting liquid slug length (*Ls*), JL, and slug length fluctuations, as formulated in Equation 9.

$$\ln\, L_S = -0.6220 - 0.2885\ln J_L - 0.2405\ln(|\text{Fluctuations}| + 1) \qquad (9)$$

This equation shows that slug length is negatively correlated with JL and slug length fluctuations. This means that as JL increases, slug length decreases, which is consistent with the phenomenon of slug fragmentation due to increased shear forces and turbulence. Furthermore, fluctuations in slug length also contribute to shortening the slug length, as greater variation in the slug structure indicates a higher degree of instability in the flow.

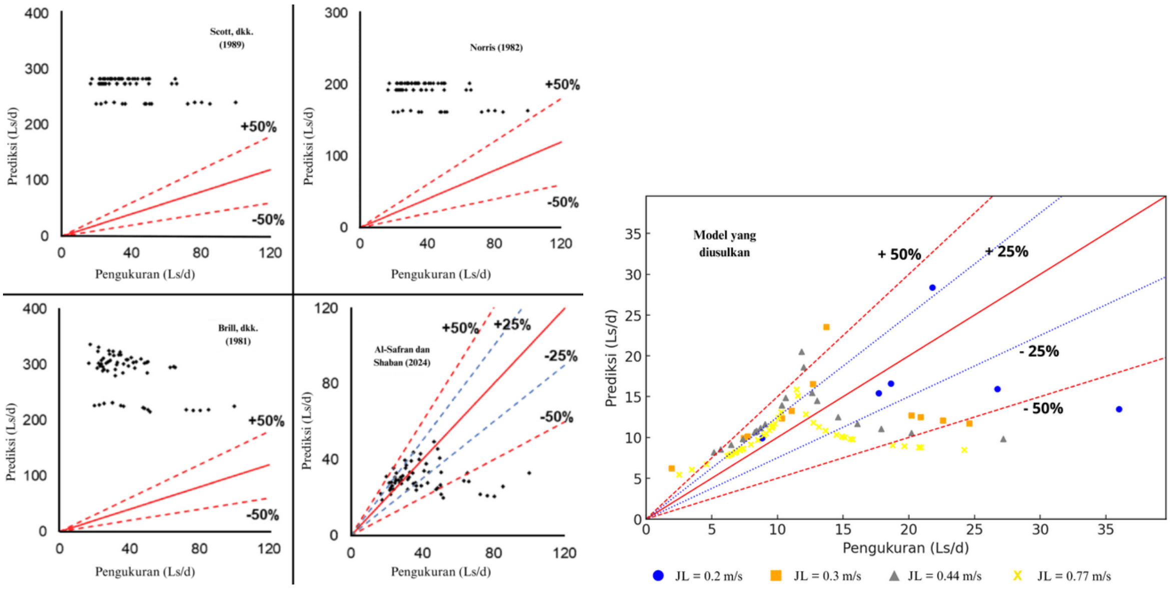

Figure 8. Comparison of Model and Validation of Slug Length against Laboratory Data

For validation, experimental data from various JL conditions were compared with model predictions. The red central line shows perfect agreement between predictions and experimental data, while the ±50% and ±25% boundary lines are used to evaluate the deviation between the model and experimental results. In the proposed model graph, most data points fall within the ±25% error margin, indicating that the model has a fairly good accuracy. In comparison, validation of the model against previous models, such as Scott et al. (1989), Norris (1982), and Brill et al. (1981), shows that the older models tend to over-predict slug length, particularly at lower slug length measurement values. This is evident from the experimental data concentrated above the +50% line, indicating that previous models were less accurate in capturing the phenomenon of slug shortening due to increased JL and fluctuations. On the other hand, the model by Al-Safran and Shaban (2024)(E. Al-Safran & Shaaban, 2024) offers better accuracy compared to earlier models but still shows considerable data dispersion outside the ±25% range.

Compared to previous models, the model proposed in this study is able to represent the relationship between slug length, JL, and slug length fluctuations. The relatively high accuracy of this model demonstrates that fluctuations play a significant role in determining slug length, an aspect that was less accounted for in previous models. Therefore, the model developed in this study provides a more comprehensive and realistic representation of the slug length dynamics in two-phase air-water flow.

D. CONCLUSIONS AND SUGGESTIONS

This study investigates the effect of liquid superficial velocity (JL) on the dynamics of liquid slug length in two-phase air-water flow within a horizontal pipe. The experimental results show that an increase in JL leads to a reduction in slug length and an increase in slug frequency due to intensified shear forces and turbulence. At low JL, the slugs tend to be longer with high variation, whereas at high JL, the slugs become shorter and more uniform. The analysis of slug length distribution indicates that the log-normal model can represent the distribution trend well, especially at high JL, where slug fragmentation is more dominant. The validation of the developed empirical model shows that most of the experimental data fall within a ±25% error margin, thereby successfully accommodating JL, fluctuation, and liquid slug length parameters, which were previously underrepresented in earlier models.

Additionally, the average length of the liquid slug is 60% smaller compared to the maximum length of the liquid slug and will never exceed this value, whereas the minimum slug length can decrease up to 630% of the average length. This phenomenon indicates a natural limit in slug growth as well as the potential for extreme fragmentation under certain conditions, opening opportunities for further research on the factors influencing the slug length limit. This study provides comprehensive insights into the dynamics of slug length in two-phase flow and results in a predictive model that can be used to estimate slug length based on JL and its fluctuations. These findings are expected to serve as a foundation for future studies related to slug flow characteristics in gas-liquid two-phase systems.

ACKNOWLEDGMENTS

The authors would like to thank DRPTM, Direktorat Jenderal Pendidikan Tinggi, Riset, dan Teknologi, Kemendikbudristek RI for their funding support through Penelitian Pendidikan Magister menuju Doktor untuk Sarjana Unggul, with contract numbers 048/E5/PG.02.00.PL/2024 and 2820/UN1/DITLIT/PT.01.03/2024, as well as the PMDSU scholarship provided to the authors. This support has greatly contributed to the successful completion of this research and the academic journey of the authors. It is hoped that the results obtained will contribute to the nation and the development of knowledge, particularly in the field of multiphase flow.

REFERENCES

Al-Safran, E. M., Gokcal, B., & Sarica, C. (2013). Investigation and Prediction of High-Viscosity Liquid Effect on Two-Phase Slug Length in Horizontal Pipelines. *SPE Production and Operations*, *28*(3), 296–305. https://doi.org/10.2118/150572-pa

Al-Safran, E., & Shaaban, O. (2024). Prediction of slug length distribution in horizontal large-diameter gas/liquid pipeline systems. *Geoenergy Science and Engineering*, *240*(December 2023), 212985. https://doi.org/10.1016/j.geoen.2024.212985

Baba, Y. D., Aliyu, A. M., Archibong, A. E., Abdulkadir, M., Lao, L., & Yeung, H. (2018). Slug length for high viscosity oil-gas flow in horizontal pipes: Experiments and prediction. *Journal of Petroleum Science and Engineering*, *165*(February), 397–411. https://doi.org/10.1016/j.petrol.2018.02.003

Brill, J. P., Schmidt, Z., Coberly, W. A., Herring, J. D., & Moore, D. W. (1981). Analysis of Two-Phase Tests in Large-Diameter Flow Lines in Prudhoe Bay Field. *Society of Petroleum Engineers Journal*, *21*(3), 363–378. https://doi.org/10.2118/8305-PA

Budiana, E. P., Pranowo, Indarto, & Deendarlianto. (2020). The meshless numerical simulation of Kelvin–Helmholtz instability during the wave growth of liquid–liquid slug flow. *Computers and Mathematics with Applications*, *80*(7), 1810–1838. https://doi.org/10.1016/j.camwa.2020.08.006

Deendarlianto, Andrianto, M., Widyaparaga, A., Dinaryanto, O., Khasani, & Indarto. (2016). CFD Studies on the Gas-Liquid Plug Two-Phase Flow in a Horizontal Pipe. *Journal of Petroleum Science and Engineering*, *147*(2), 779–787. https://doi.org/10.1016/j.petrol.2016.09.019

Deendarlianto, Rahmandhika, A., Widyatama, A., Dinaryanto, O., Widyaparaga, A., & Indarto. (2019). Experimental study on the hydrodynamic behavior of gas-liquid air-water two-phase flow near the transition to slug flow in horizontal pipes. *International Journal of Heat and Mass Transfer*, *130*, 187–203. https://doi.org/10.1016/j.ijheatmasstransfer.2018.10.085

Dinaryanto, O., Prayitno, Y. A. K., Majid, A. I., Hudaya, A. Z., Nusirwan, Y. A., Widyaparaga, A., … Deendarlianto. (2017). Experimental investigation on the initiation and flow development of gas-liquid slug two-phase flow in a horizontal pipe. *Experimental Thermal and Fluid Science*, *81*, 93–108. https://doi.org/10.1016/j.expthermflusci.2016.10.013

Kusumaningsih, H., Indarto, & Deendarlianto. (2025). The effect of flow pattern on the heat transfer performance during the transportation of gas-Newtonian/non-Newtonian liquids two-phase flow in a horizontal microchannel. *International Communications in Heat and Mass Transfer*, *161*(2), 108507. https://doi.org/10.1016/j.icheatmasstransfer.2024.108507

Mandhane, J. M., Gregory, G. A., & Aziz, K. (1974). A flow pattern map for gas—liquid flow in horizontal pipes. *International Journal of Multiphase Flow*, *1*(4), 537–553. https://doi.org/10.1016/0301-9322(74)90006-8

Norris, L. (1982). *Correlation of Prudhoe Bay Liquid Slug Lengths and Holdups Including 1981 Large Diameter Flowline Tests*. Houston, Texas.

Scott, S. L., Shoham, O., & Brill, J. P. (1989). Prediction of Slug Length in Horizontal, Large-Diameter Pipes. *SPE Production Engineering*, *4*(3), 335–340. https://doi.org/https://doi.org/10.2118/15103-PA

Setyawan, A., Indarto, & Deendarlianto. (2016). The effect of the fluid properties on the wave velocity and wave frequency of gas-liquid annular two-phase flow in a horizontal pipe. *Experimental Thermal and Fluid Science*, *71*, 25–41. https://doi.org/10.1016/j.expthermflusci.2015.10.008

Setyawan, A., Indarto, & Deendarlianto. (2017). Experimental investigations of the circumferential liquid film distribution of air-water annular two-phase flow in a horizontal pipe. *Experimental Thermal and Fluid Science*, *85*, 95–118. https://doi.org/10.1016/j.expthermflusci.2017.02.026

Shaaban, O. M., & Al-Safran, E. M. (2023). Prediction of slug length for high-viscosity oil in gas/liquid horizontal and slightly inclined pipe flows. *Geoenergy Science and Engineering*, *221*(November 2022), 211348. https://doi.org/10.1016/j.geoen.2022.211348

Wang, S. (2012). *Experiments and Model Development for High-Viscosity Oil/Water/Gas Horizontal and Upward Vertical Pipe Flows*. The University of Tulsa.

Widyatama, A., Dinaryanto, O., Indarto, & Deendarlianto. (2018). The development of image processing technique to study the interfacial behavior of air-water slug two-phase flow in horizontal pipes. *Flow Measurement and Instrumentation*, *59*(November 2016), 168–180. https://doi.org/10.1016/j.flowmeasinst.2017.12.015

Wijayanta, S., Deendarlianto, Indarto, Prasetyo, A., & Hudaya, A. Z. (2023). The effect of the liquid physical properties on the wave frequency and wave velocity of co-current gas-liquid stratified two-phase flow in a horizontal pipe. *International Journal of Multiphase Flow*, *158*(2), 104300. https://doi.org/10.1016/j.ijmultiphaseflow.2022.104300

Wijayanta, S., Indarto, Deendarlianto, Catrawedarma, I. G. N. B., & Hudaya, A. Z. (2022). Statistical characterization of the interfacial behavior of the sub-regimes in gas-liquid stratified two-phase flow in a horizontal pipe. *Flow Measurement and Instrumentation*, *83*(2), 102107. https://doi.org/10.1016/j.flowmeasinst.2021.102107

Yeoh, G. H., & Joshi, J. B. (2023). *Handbook of Multiphase Flow Science and Technology*. Singapore: Springer Nature Singapore Pte Ltd. https://doi.org/https://doi.org/10.1007/978-981-287-092-6

Zheng, D., Che, D., & Liu, Y. (2008). Experimental investigation on gas-liquid two-phase slug flow enhanced carbon dioxide corrosion in vertical upward pipeline. *Corrosion Science*, *50*(11), 3005–3020. https://doi.org/10.1016/j.corsci.2008.08.006